Singlet Oxygen Detection: A Review of Recent Advances

Lyubov Eratova[1], Elena Zharkikh[1], Edik Rafailov[2], and Viktor Dremin[1,2*]

[1] Research and Development Center of Biomedical Photonics, Orel State University, 95 Komsomolskaya str., Orel 302026, Russian Federation

[2] Aston Institute of Photonic Technologies, Aston University, Birmingham, B4 7ET, United Kingdom

*e-mail: dremin_viktor@mail.ru

Abstract. As part of the search for and development of an optimal solution related to singlet oxygen ($^1O_2$) detection, an analytical review of research in this direction was carried out. $^1O_2$ is one of the key participants in many biological processes, so its detection and numerical estimation are the subject of a close study by many research groups. To date, several approaches to the optical detection of $^1O_2$ have been proposed, in most cases based on the registration of $^1O_2$ luminescence in the near-infrared range of the spectrum. The review also presents various fluorescence probes, chemical traps and several other tools that are also used for $^1O_2$ detection.

Keywords: singlet oxygen; luminescence detection; probes; chemical traps; electron paramagnetic resonance spectroscopy (EPR); quantitative PCR (qPCR).

1 Introduction

Today, one of the developing fields of biology is redox biology, which aims to study reactive oxygen species (ROS). Singlet oxygen ($^1O_2$) is one of the most reactive forms of ROS. $^1O_2$, discovered and named by Herzberg [1] in 1934, is a product of the activation of the triplet state of molecular oxygen ($^3O_2$). It is generated through photochemical reactions, for example, when light is absorbed by photosensitizers (PS) or during metabolic processes in mitochondria and chloroplasts. Its high reactivity allows it to interact with lipids, proteins, and nucleic acids, causing their oxidation and damage. At the same time, $^1O_2$ is involved in the regulation of cellular signaling pathways, such as apoptosis and autophagy, highlighting its dual role in the cell [2−3].

Particular interest in $^1O_2$ is due to its key role in photodynamic therapy (PDT) of malignant tumors, where it is used to selectively destroy cancer cells [4−6]. Selectively means that photosensitizer is accumulated in tumor tissue and does not affect healthy tissue in a destructive manner. Upon irradiation with light of a specific wavelength, the PS generates $^1O_2$, which induces localized oxidative damage, leading to cancer cell death via apoptosis, necrosis, or vascular shutdown. In addition, its antimicrobial properties have applications in the development of new disinfection methods [7]. In industry and organic synthesis, $^1O_2$ is used for the selective oxidation of complex molecules, which allows the creation of new materials and pharmaceutical compounds. However, despite its obvious benefits, its use is associated with a number of challenges and limitations.

The main difficulty lies in the generation of $^1O_2$. In nature, it can be produced by ultraviolet radiation, during photosynthesis and by some enzymes. In laboratory and industrial conditions, it is produced with the help of photosensitizers – compounds capable of transferring energy to molecular oxygen, converting it to the singlet state – or directly, at excitation wavelengths of triplet oxygen [8]. However, the efficiency of such processes depends on many factors, including the type of sensitizer, the wavelength of light used, and the environment in which the reaction takes place [7]. The detection of $^1O_2$ is no less challenging. Because of its short lifetime (nanoseconds to microseconds, depending on the medium) and high chemical activity, direct detection is difficult. Thus, despite the high interest in $^1O_2$, issues related to its generation, stability, and detection remain unresolved. Modern research is aimed at developing more efficient methods for its generation and accurate detection, which will open new opportunities for the application of this unique compound in medicine, biotechnology and industry.

This review discusses methods for its detection and the existing problems that hinder their effective use in various fields of science and techniques.

2 Singlet Oxygen Luminescence Detection

2.1 Historical Overview

After its formation, a molecule of $^1O_2$ can undergo nonradiative decay, oxidize surrounding biomolecules or undergo radiative decay at around 1270 nm. The detection of this near-infrared (NIR) emission through time-resolved techniques is a widely employed approach for assessing the lifetimes and quantum yields of $^1O_2$.

$^1O_2$ emits ultra-weak luminescence at around 1270 nm as it relaxes from its excited state to the ground state. This radiative transition is spin-forbidden, resulting in a very low quantum yield (typically 10^{-6} to 10^{-8}) and, consequently, low emission intensity [9]. The lifetime of $^1O_2$ varies with the surrounding medium, ranging from tens of microseconds in the gas phase to less than a microsecond in biological environments. Given the possible concentrations of $^1O_2$ generated [10], the absolute intensity of its luminescence is extremely low, typically in the femtowatt (10^{-15} W) to picowatt (10^{-12} W) range. At the same time, even lower values should be expected with direct optical generation.

The first studies in the field of time-resolved detection of $^1O_2$ based on the luminescence properties were undertaken by Krasnovsky's group back in 1976 [11]. The approach developed in this work is by now considered to be the standard approach for the study of $^1O_2$ photochemistry. $^1O_2$ phosphorescence was studied in pigment solutions containing no hydrogen atoms, and spectrometers with mechanical phosphoroscopes and a photodetector system based on cooled photomultiplier tubes were used for its registration. The excitation, emission, and luminescence lifetime spectra of $^1O_2$ were studied [12] (see Fig. 1).

Over the years, several teams have attempted to measure $^1O_2$ levels under conditions that approximate physiological conditions. For example, B. Roider et al. demonstrated time-resolved emission experiments to detect $^1O_2$ luminescence in a suspension of haemolysed erythrocytes [13]. However, separating the useful signal from the strong background emission required a careful approach in the selection of the sensitiser, optimisation of the detection system, use of D_2O as solvent and sodium azide as a quencher, and variation of the O_2 concentration. Thus, the demonstrated approach did not allow adequate measurement of $^1O_2$ under physiological experimental conditions *in vitro* or *in vivo*.
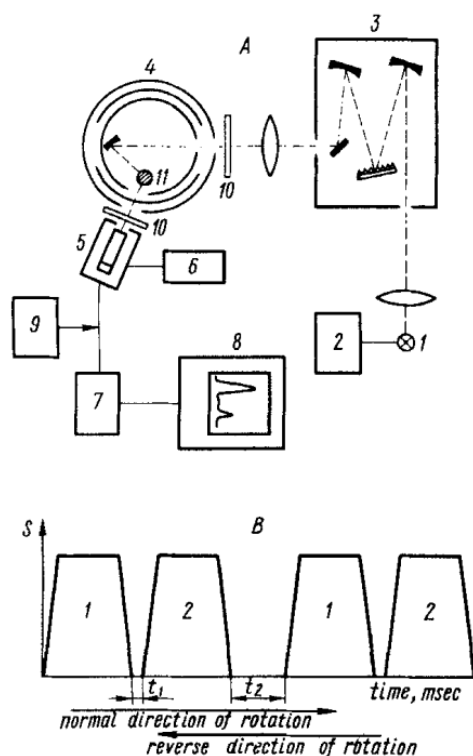

Fig. 1 (A) Block-scheme of the apparatus for measuring excitation spectra of the 1O2 luminescence: (1) Xe lamp 1000 W, (2) power supply, (3) grating monochromator, (4) phosphoroscope, (5) photomultiplier, (6) high voltage supply, (7) direct current amplifier, (8) chart recorder, (9) oscilloscope (to monitor the speed of rotation), (10) light filters, (11) sample holder. (B) Sequence and time course of opening and closing the phosphoroscope holes: (1) the phase of excitation, (2) the phase of luminescence measurement. tl and t2 are dark intervals, S is the area of the holes opened for the passing of light [12]. Reproduced with permission of John Wiley and Sons.
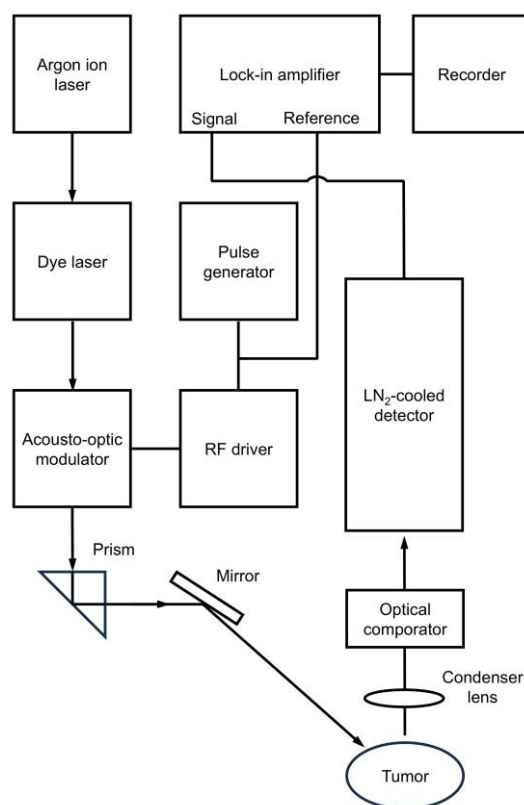

Fig. 2 Schematic diagram of apparatus used to detect $^1O_2$ emission from a laser-irradiated SMT-F tumor implanted subcutaneously in a type-DBA/2 mouse. Mouse had been previously injected intrapentoneally with Photofrin II at a level of 50 mg/kg. Incident laser power was typically 20 mW and the wavelength set at 630 nm. Adopted from Ref. [14].
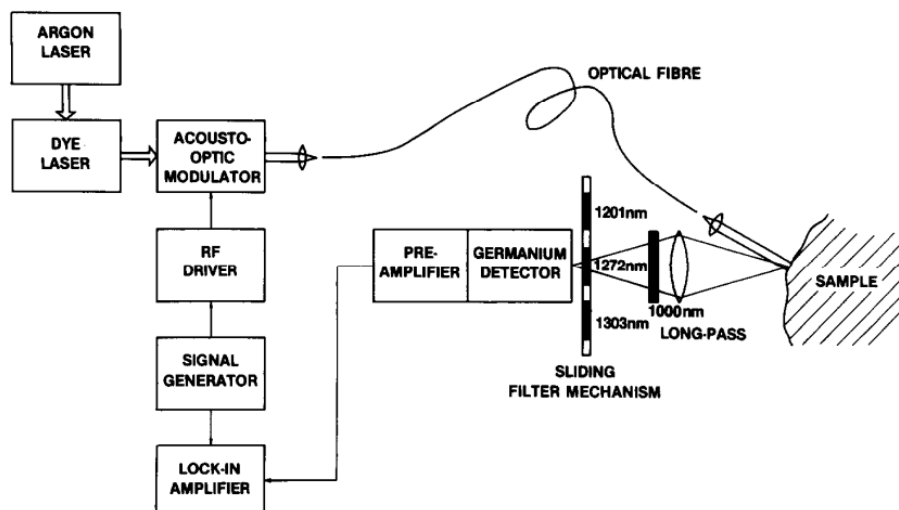
Fig. 3 Schematic diagram of apparatus for the detection of $^1O_2$ luminescence *in vivo*. The sliding filter mechanism facilitates the quadrature detection method and allows rough verification of the luminescence spectrum. For *in vitro* experiments, a quartz cuvette (1 cm) was used, and samples were irradiated through the side face [15]. Reproduced with permission of Elsevier.
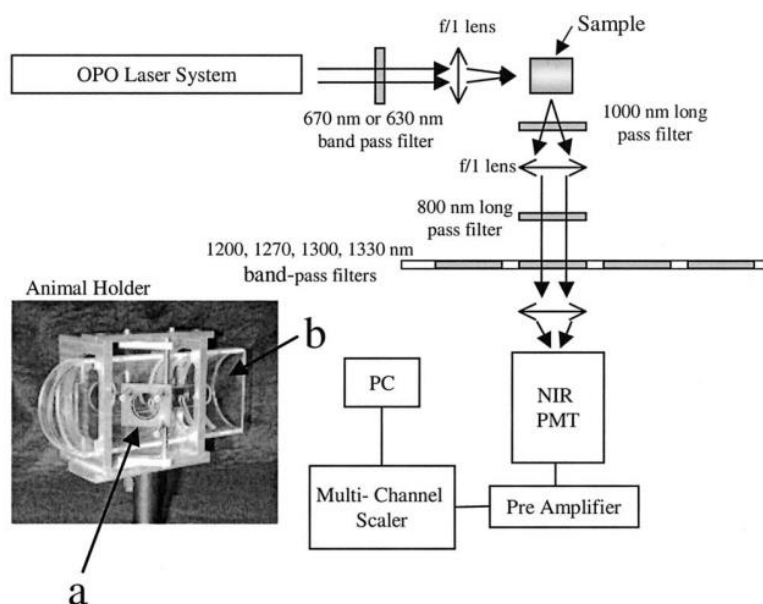

Fig. 4 Schematic of the experimental system used for $^1O_2$ luminescence detection. Inset: purpose-built animal holder used for *in vivo* experiments. Excitation light was delivered through the circular port (a), and measurements were made through a second port at 90° (not seen). The animal was held in the hemispheric cylinder (b) [16]. Reproduced with permission of John Wiley and Sons.

The multiple shortening of the lifetime of $^1O_2$ in cells and tissues (Figs. 2−3), caused by its rapid quenching by biomolecules, and the lack of sufficiently sensitive detectors in the near-infrared wavelength range have long prevented the development of an approach to measuring $^1O_2$ levels under physiological conditions that would give consistent results [14, 15].

In 2002, a group of researchers led by B. S. Wilson proposed the use of near-infrared luminescence measurement during photodynamic therapy as a valuable tool for direct dosimetric assessment of changes in $^1O_2$ levels [16]. The experimental setup, which is shown in

Fig. 4, included the use of a tunable pulsed Nd:YAG laser, 4 bandpass filters with maximum transmission in the range of 1200, 1270, 1300 and 1330 nm and a photodetector based on the use of a liquid nitrogen cooled photomultiplier tube, which allows extremely sensitive detection in the range of 1200−1330 nm and has a fast response time. The authors performed experiments with photosensitiser solutions, *in vitro* studies using cell suspension, and *in vivo* studies on Wistar rats with generation and measurement of $^1O_2$ in skin and liver surface areas.
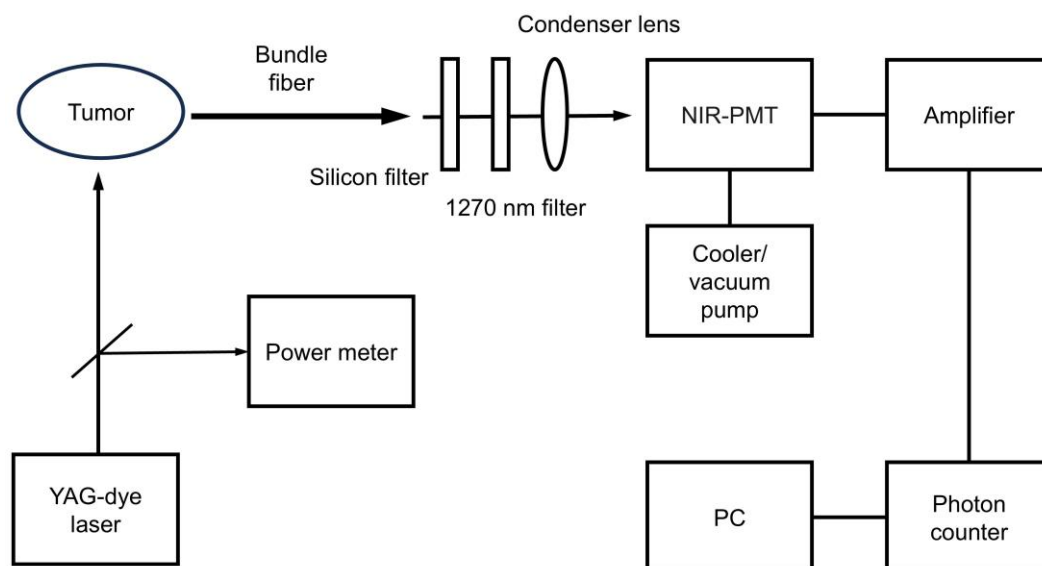
Fig. 5 Schematic drawing of the experimental setup for *in vitro* and *in vivo* monitoring of $^1O_2$. Adapted from Ref. [20].

The study showed that the application of the approach developed by the authors provided convincing evidence that $^1O_2$ luminescence from an intracellular photosensitiser could be detected and quantified in cell suspension in an H_2O-based medium and in tissues of laboratory animals *in vivo*. Later, the proposed approach was repeatedly applied in studies of $^1O_2$ generation efficiency in photodynamic therapy of implanted murine tumours sensitized with ATX-S10 [17], killing OCI-AML5 leukaemia cells treated with aminolevulinic acid (ALA) induced protoporphyrin IX (PpIX) [18, 19], and in the evaluation of PDT efficiency in an experimental model of glioma sensitised with methylene blue (see Fig. 5) [20].

Li et al. used an approach based on the use of photomultiplier tubes with high sensitivity in the NIR range to measure the time-resolved luminescence of $^1O_2$ and an optical filtering system to increase the sensitivity of $^1O_2$ detection [21]. A bifurcated optical probe was used to deliver pulsed laser light and collect $^1O_2$ emission, which facilitates the application of the system in *in vivo* experiments. Since the detected emission includes both the $^1O_2$ luminescence signal and other possible NIR emissions such as photosensitiser fluorescence, tissue phosphorescence and autofluorescence, etc., for spectral separation of $^1O_2$ radiation from interference, the recorded near-IR radiation was passed through a series of three narrow-band filters with a bandwidth of 15 nm and central wavelengths of 1220, 1270, and 1315 nm. The peak of $^1O_2$ luminescence was centred in the 1270 ± 10 nm wavelength region. Two filters centred at 1220 and 1315 nm provided background emission measurements that did not contain $^1O_2$ emission. Data were recorded by a thermoelectrically cooled photomultiplier tube operating in photon counting mode, after which the signal was amplified and processed by a data acquisition system. The authors tested their $^1O_2$ detection method on rat tumours during PDT, using the prostate cancer cell line R3327-MatLyLu as an animal model. The $^1O_2$ measurement sensor was placed 1.5 mm above the skin of the animals. The study protocol included recording $^1O_2$ emission before administration of the photosensitiser, just before the start of therapeutic light irradiation after the photosensitiser had spread systemically during a defined period of its incubation, several times during the therapeutic irradiation and at the end of light irradiation. The authors observed tumour regression that correlated with the measured level of $^1O_2$ production. The results of the study demonstrated a moderate signal-to-noise ratio and established a clear relationship between $^1O_2$ production and tumour shrinkage.

2.2 Recent Advances

However, the *in vivo* measurement of $^1O_2$ luminescence using photomultiplier tubes presents a number of problems since this type of photodetector has low efficiency and is highly sensitive to noise and external illumination, which prevents effective detection of luminescence in biological tissues with low emission and short lifetime (<<1 ms). To overcome this problem, some teams of authors have turned to new technologies based on the use of superconducting single-photon detectors, which offer high sensitivity in the IR region, picosecond time resolution and low dark noise. The group of Hadfield et al. [22] proposed the first application of superconducting nanowire single-photon detectors for $^1O_2$ detection. In their study, $^1O_2$ emission was recorded using time-resolved and spectrally filtered measurements performed in a solution of Rose Bengal (RB). The study demonstrated the quenching of $^1O_2$ luminescence by sodium azide. Subsequently, bovine serum albumin (BSA) was used to mimic a biological medium containing the protein; with increasing BSA concentration, the evolution of the RB triplet lifetime and singlet state of $^1O_2$ were successfully observed. As expected, the lifetime of the RB triplet state increased

markedly upon binding to the protein, which is probably due to the shielding of the photosensitizer from the diffusion of oxygen molecules with which the triplet state can react. A decrease in the lifetime of $^1O_2$ was also observed in the studies performed and was attributed to the quenching of $^1O_2$ luminescence emission by the protein. The authors also demonstrated an optical fibre delivery and data acquisition scheme, which is particularly important in the field of $^1O_2$ detection for preclinical and clinical *in vivo* applications, which is shown in Fig. 6.

Alternative low-cost approaches to $^1O_2$ detection have been proposed in the work [23]. The authors developed a tool for measuring $^1O_2$ luminescence using an InGaAs avalanche photodiode and simple electronics. This approach was tested in organic solvents such as tetrachloromethane (CCl4), ethanol, and DMSO. The authors have demonstrated spectrally resolved measurements of $^1O_2$ luminescence in CCl4 using the developed setup, showing high complementarity with literature data on $^1O_2$ luminescence. The authors propose to apply the setup to evaluate the efficacy of new photosensitizers as well as for $^1O_2$ dosimetry during PDT, but for the latter application, additional work is needed to improve the sensitivity of the detector in order to apply it in real systems.

Since the biological environment is characterized by high heterogeneity, the registration of time-resolved $^1O_2$ luminescence does not always provide the desired result, as it may represent an average value for many very different deactivation processes. In this regard, the development of spatially resolved detection methods is of interest. The first steps in this field were made by the group of Ogilby et al. [24−26]. Using wide-field microscopy, they were able to detect the luminescence of $^1O_2$ in neurons produced by the photosensitizer TMPyP and obtained data on the typical distances over which $^1O_2$ diffuses inside cells. In the detection system developed by this group, the luminescence of the samples is collected by a microscope objective and passed through the same dichroic optics used to reflect Xe-lamp light. Spectral discrimination of $^1O_2$ phosphorescence in the near-IR is achieved using an interference filter centered at 787 nm, after which the emission is fed to a custom-built detector with a linear array of InGaAs photodiodes operating at −100 °C. The detector contains 512 elements (pixels), each with a size of 50×50 μm. The spatial resolution available in this experiment is determined by a combination of the size of the detector array elements and the magnification of the objective lens. For data recorded with a 20× objective lens, the authors obtained a resolution of up to 2.5 μm.
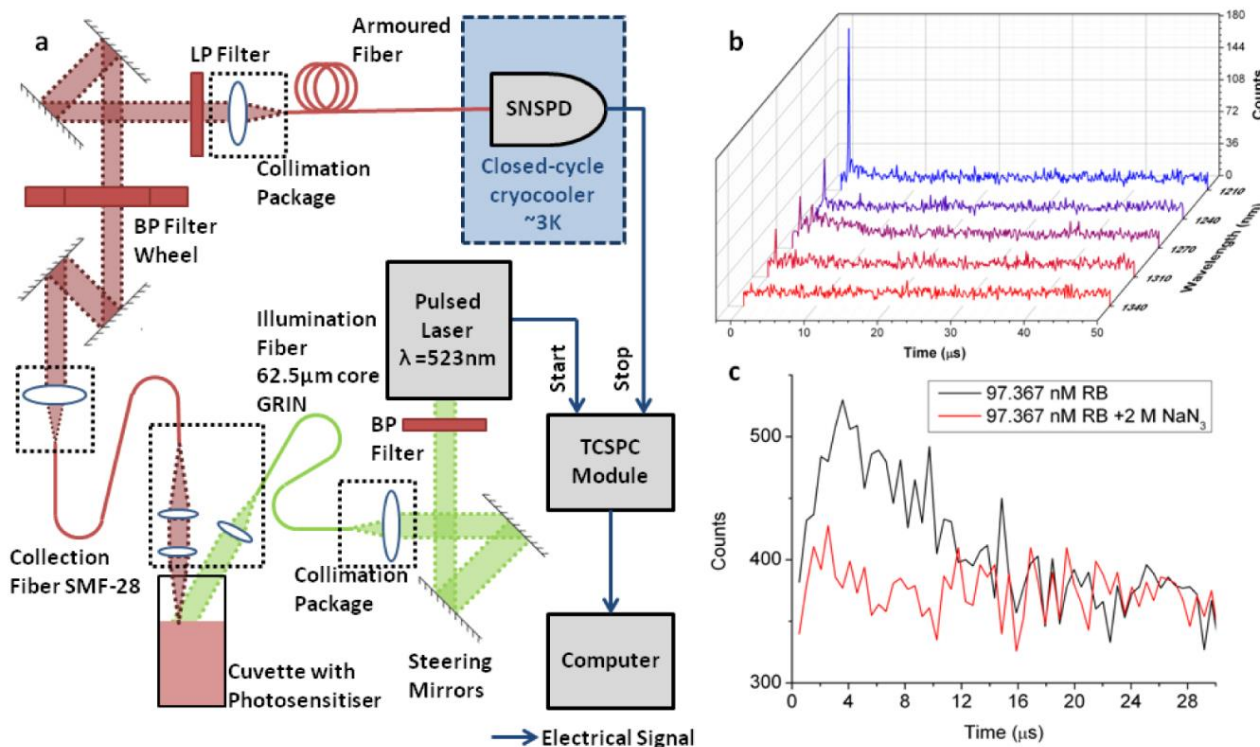

Fig. 6 (a) Fiber-based delivery and collection for $^1O_2$ luminescence detection: schematic of the experimental setup, (b) luminescence time histograms in RB (97.367 nM) for the different bandpass filters (30 min acquisition time, 0.128 μs bin size), (c) quenching with sodium azide [60 min acquisition time, 0.512 μs bin size] [22]. Optica Publishing Group Open Access Publishing Agreement.
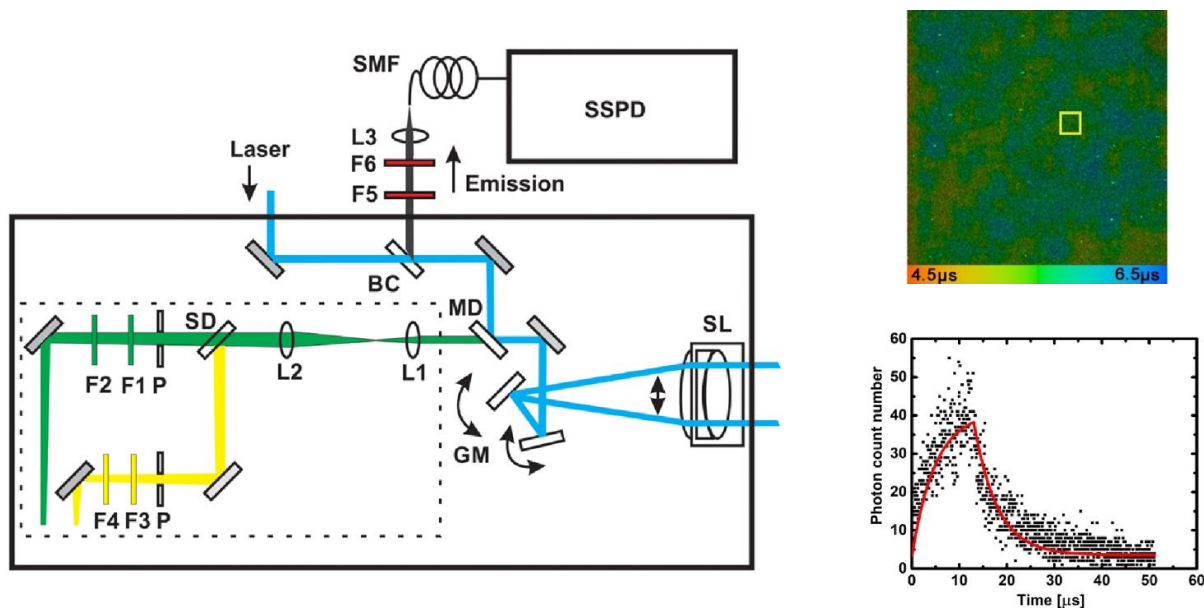
Fig. 7 Left part: Schematic of the experimental setup for $^1O_2$ measurements. SSPD: superconducting single-photon detector; SMF: single-mode fiber; BC: beam combiner 810LP; P: pinhole; F1, F3: long-pass filters; F2, F4: bandpass filters; F5: long-pass filter 830LP; F6: bandpass filter 1260/30. GM: galvo-mirrors; SL: scanning lens; MD: main dichroic mirror. The dashed line shows a part of the scanner that may be used for confocal detection of fluorescence from a sample. Right part (top): phosphorescence lifetime image (256×256 pixels) of $^1O_2$ in the solution of Ce6. The full scanned field corresponds to 200 µm. Right part (bottom): time-resolved kinetics of the phosphorescence in the selected spot, marked with a square on the image. Excitation wavelength: 405 nm. Collection time: 600 s [27]. Reproduced with permission of Optica Publishing Group.

Another example of the study of $^1O_2$ distribution in cell culture and time-resolved measurement of its luminescence is the work of Shcheslavskiy's group [27], which presents a system based on a superconducting single-photon detector coupled to a confocal scanner modified for NIR measurements. The recording of the $^1O_2$ phosphorescence signal at 1270 nm was performed using time-correlated single photon counting (TCSPC). The system was verified by performing experiments both on solutions of photosensitizers frequently used in photodynamic therapy – Cle6 and methylene blue – and on HeLa cells (Fig. 7).

The paper demonstrates the ability of the system to record the lifetime distribution of $^1O_2$ luminescence over an image; however, the data acquisition time in this system is rather long due to the low quantum yield of $^1O_2$ luminescence and the rapid quenching of $^1O_2$ in the cells. The authors propose to use a fluorescence image of an object to find the region of interest and then record $^1O_2$ luminescence kinetics only from specific points in the image to circumvent this problem of long data acquisition time.

The research team of Hackbarth et al., in their paper [28], studied the $^1O_2$ luminescence kinetics in tumour cells of a mouse model *in vivo*. The time-correlated multiple photon counting (TCMPC) method in the NIR region with central wavelengths of 1200, 1270 and 1340 nm was used to record $^1O_2$ phosphorescence *in vivo*. The authors studied the dynamics of changes in $^1O_2$ phosphorescence during PDT of a cancer tumour model obtained by subcutaneously implanting the S180

sarcoma cell line into laboratory animals. The study showed a very weak $^1O_2$ phosphorescence signal *in vivo* in contradiction to the parallel results obtained on cell culture *in vitro*, which they believe may be due to oxygen depletion even at moderate (on the scale of PDT) illumination intensity, shortly after the start of illumination.

Although the new technologies being developed look extremely promising, optical detection methods suffer from a low level of $^1O_2$ luminescence emission and its rapid attenuation, so the quantitative detection of very small concentrations of $^1O_2$, especially with direct optical generation [8], is currently very difficult, which is especially critical when conducting *in vivo* studies.

3 Singlet Oxygen Detection Using Probes

Various probes are also used to detect $^1O_2$, which can be divided into three main groups: absorption-based probes, photoluminescent probes and chemiluminescent probes [29]. Probes for $^1O_2$ detection must meet a number of requirements, including sensitivity, fast response time, selectivity with respect to other ROS. Moreover, reversibility may be advantageous in specific scenarios (e.g., real-time continuous monitoring of $^1O_2$ dynamics), but it should not necessarily be prioritized over robustness and detection limits. Additionally, water-solubility is a practical necessity for biological studies, as many $^1O_2$ reactions occur in aqueous media. Probes used to detect $^1O_2$ in biological media must also meet additional conditions. They should have low cytotoxicity and sufficient dynamics to register rapid processes [26, 29, 30].
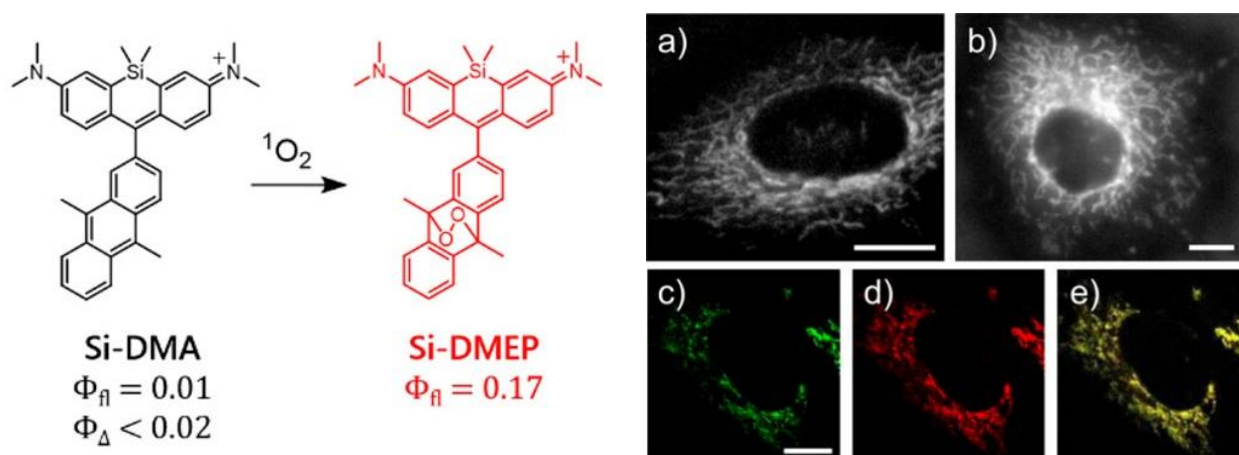
Fig. 8 Left part: chemical structures of Si-DMA, its peroxidized product (Si-DMEP). Right part: Example of HeLa cells stained with [Si-DMA] = (a) 20 and (b) 100 nM for 1 h. Colocalization test of Si-DMA in mitochondria (c−e). (c) MitoTracker Green and (d) [Si-DMA] = 100 nM. Clear colocalizations of two dyes are observed in the merged image (e), and the intensities of each image have been adjusted to obtain a clear picture. Scale bar = 10 μm (B) [31]. Reproduced with permission of American Chemical Society.

Majima et al. synthesized a new far-red fluorescence probe (excitation/emission maxima at 640/670 nm) composed of silicon-containing rhodamine and anthracene moieties, namely Si-DMA, as a chromophore and a $^1O_2$ reactive site, respectively [31]. In the presence of $^1O_2$, the fluorescence of Si-DMA increases 17 times due to endoperoxide formation at the anthracene moiety (Fig. 8). Among seven different ROS, Si-DMA is able to selectively detect the $^1O_2$. In addition, Si-DMA is able to visualize the real-time generation of $^1O_2$ from protoporphyrin IX in mitochondria with 5-aminolevulinic acid (5-ALA), a precursor of heme. This dye makes it possible to visualize $^1O_2$ generated during PDT with a spatial resolution of a single mitochondrial tubule.

Over the past few decades, the photoinduced electron transfer (PET) process has become widespread for the development of selective probes for $^1O_2$ detection. The anthracene link is commonly used as the central core of the fluorophore in the construction of PET-based probes due to its rapid reaction with $^1O_2$ [32]. The Singlet Oxygen Sensor Green (SOSG) is a widely recognized and commercially available $^1O_2$ detection probe. The SOSG molecule consists of two parts: a fluorophore and an anthracene-derived trapping moiety. In the absence of $^1O_2$, emission from the fluorophore is quenched by electron transfer from the adjacent trapping moiety. The indicator exhibits weak blue fluorescence with excitation/emission maxima at 372/395 and 393/416 nm. In an environment containing $^1O_2$, the trapping moiety reacts with $^1O_2$ and forms an endoperoxide (EP) anthracene, which is no longer an efficient intramolecular electron donor (see Fig. 9). Removing the quenching leads to the fluorophore's fluorescence at excitation/emission maxima of about 504/525 nm [33].
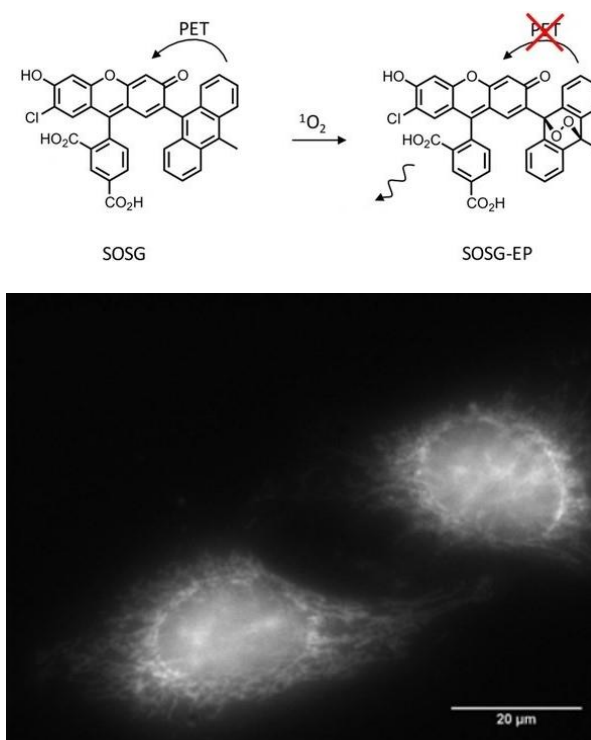

Fig. 9 Top part: chemical structure of SOSG and the formation of SOSG-EP upon interaction with $^1O_2$, leading to activation of fluorescence output. Bottom part: Image of two HeLa cells based on the fluorescence of SOSG. Data were recorded after 2 h incubation, in the dark, in our standard maintenance medium into which SOSG had been dissolved. The nuclei are visible as the large oval structures, and SOSG-containing filamentous structures in the cytoplasm clearly extend out to the cell membrane [33]. Reproduced with permission of John Wiley and Sons.

However, the ability of SOSG to penetrate cell membranes is still an open question [34]. Some studies have shown that SOSG can be absorbed by cells in stressful situations or in the absence of proteins. Work [35] demonstrates that different microbial species and cancer cells become fluorescent when exposed to SOSG under conditions which exclude the generation of $^1O_2$. Cells permeabilized with chlorhexidine or by heat exposure under anaerobic conditions exhibited SOSG fluorescence. A number of authors claim that this probe is not suitable for most biological purposes [36]. Also, when using SOSG in tissue slices, there is a slight increase in the fluorescence intensity during $^1O_2$ generation. One of these limitations is the short lifetime of $^1O_2$, which leads to a higher probability of alternative interactions occurring at a higher rate. This is due to the significant reaction rate constant and the relatively low operating concentration of SOSG. As a result, these interactions can weaken or completely prevent the reaction between $^1O_2$ and SOSG necessary for the formation of a fluorescent product [37]. To increase biocompatibility, SOSG is covalently linked to a polyacrylamide nanoparticle core using different architectures. NanoSOSG is easily absorbed by cells, and at the same time, the spectral characteristics do not change inside the cells, and the intracellularly generated $^1O_2$ probe reacts with an increase in fluorescence [38]. Also, the Aarhus Sensor Green (ASG) probe is an effective solution to the disadvantages of commercially available SOSG probes. Unlike SOSG, ASG includes fluorine atoms, effectively preventing self-photosensitization at physiological pH. This characteristic gives ASG a clear advantage over SOSG [39].

UV-Vis spectroscopy is also a widely used method for measuring $^1O_2$. Anthracene and benzofuran are well-known compounds with the ability to selectively absorb $^1O_2$ which is shown in Fig. 10.

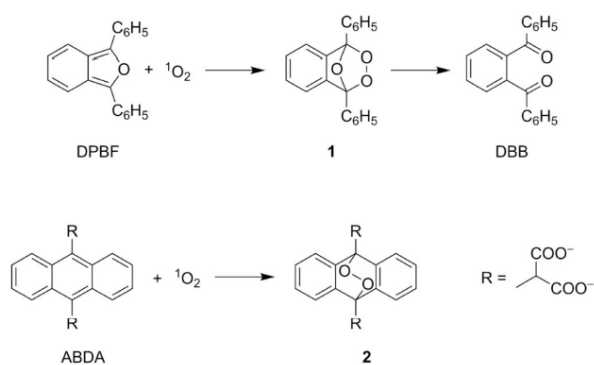Fig. 10 Reaction of $^1O_2$ with with DPBF (top) and ABDA (bottom) [40]. Creative Commons CC-BY.

When these aromatic molecules are oxidized by $^1O_2$, their absorption decreases, which allows a semi-quantitative assessment of the $^1O_2$ present. Although UV-Vis spectroscopy is less sensitive than fluorescence spectroscopy, it is less susceptible to distortion caused by impurities due to the absence of quenching [40]. For UV-Vis spectroscopy, 1,3-diphenylisobenzofuran (DPBF) is one of the most commonly used probes for $^1O_2$ detection [41]. DPBF can also be used in fluorescence spectroscopy due to its strong fluorescence signal. However, DPBF is a water-insoluble probe, which significantly limits its application to biological media.

4 Other Possible Approaches

One of the detection methods is also the use of chemical "traps", for example, histidine, to capture $^1O_2$ using imidazole rings to form a dioxygen complex. The decrease in the volume concentration of oxygen can be precisely controlled using an oxygen electrode (Clark electrode) [37, 42].

In addition, special spin traps have been developed that react with $^1O_2$ to form a stable nitroxide radical, which can be measured using electron paramagnetic resonance (EPR) spectroscopy [43]. The theoretical detection limit of EPR in the Bruker ELEXSYS E500 spectrometer has an approximate concentration sensitivity limit of 4.0×10^{-12} mol. However, it is worth noting that this method has certain limitations since various biomolecules can potentially interact with spin traps. Therefore, it is important to assess whether any changes have occurred in the trap. Another important factor to consider is the degree of penetration of spin traps into the tissue, since not all spin traps are equally effective under physiological pH conditions [44].

The use of real-time quantitative PCR to measure the accumulation of certain transcripts suggests the next potential method for indirectly detecting the short-term existence of $^1O_2$ [45]. Thanks to extensive research using microchip experiments, RNAseq, as well as Genevestigator databases, it has become possible to accurately identify gene markers that specifically indicate the presence of $^1O_2$ [46].

Lipid peroxidation is a key downstream effect of ROS and plays a role in cell signaling. The Thiobarbituric Acid (TBA) assay is a common method to measure lipid peroxidation by detecting malondialdehyde (MDA), though it lacks specificity [47]. Advanced techniques like high-performance liquid chromatography-electrospray ionization-tandem mass spectrometry (HPLC-ESI-MS/MS) improve specificity by distinguishing between type I (free radical) and type II ($^1O_2$) lipid peroxidation using hydroxy fatty acids (HOTEs) as markers [48].

5 Conclusion

Although the new technologies under development look very promising, both temporal and spatial resolution methods suffer from the weak emission level of $^1O_2$ luminescence and its rapid attenuation, so quantitative detection of very low concentrations of $^1O_2$ is currently very challenging, especially with direct optical generation, which is particularly critical for *in vivo* studies.

Chemical probes and traps are characterized by limited penetration into cells or tissues, which will make *in vivo* and *in vitro* studies difficult. It is also worth

considering the environmental conditions in which the probe/trap is located, for example, pH, and the specificity of the substances in question.

As we can see, the described methods have a number of limitations, but a combination of approaches can eliminate some of them. For example, the use of fluorescent probes together with optical luminescence detection can make it possible to determine the total amount of $^1O_2$ (reacted and returned to the triplet state).

Disclosures

Acknowledgements

References

1. G. Herzberg, "Photography of the Infra-Red Solar Spectrum to Wave-length 12,900 A," Nature 133(3368), 759–759 (1934).
2. I. N. Novikova, E. V. Potapova, V. V. Dremin, A. V. Dunaev, and A. Y. Abramov, "Laser-induced singlet oxygen selectively triggers oscillatory mitochondrial permeability transition and apoptosis in melanoma cell lines," Life Sciences 304, 120720 (2022).
3. V. Dremin, O. Semyachkina-Glushkovskaya, and E. Rafailov, "Direct Laser-Induced Singlet Oxygen in Biological Systems: Application From in Vitro to in Vivo," IEEE Journal of Selected Topics in Quantum Electronics 29(4: Biophotonics), 1–11 (2023).
4. J. P. Celli, B. Q. Spring, I. Rizvi, C. L. Evans, K. S. Samkoe, S. Verma, B. W. Pogue, and T. Hasan, "Imaging and Photodynamic Therapy: Mechanisms, Monitoring, and Optimization," Chemical Reviews 110(5), 2795–2838 (2010).
5. T. J. Dougherty, C. J. Gomer, B. W. Henderson, G. Jori, D. Kessel, M. Korbelik, J. Moan, and Q. Peng, "Photodynamic Therapy," JNCI Journal of the National Cancer Institute 90(12), 889–905 (1998).
6. I. Makovik, M. Volkov, L. Eratova, and V. Dremin, "Vascular targeted optical theranostics: enhanced photoplethysmography imaging of laser-induced singlet oxygen effects," Optics Letters 49(5), 1137 (2024).
7. X. Ragàs, X. He, M. Agut, M. Roxo-Rosa, A. Gonsalves, A. Serra, and S. Nonell, "Singlet Oxygen in Antimicrobial Photodynamic Therapy: Photosensitizer-Dependent Production and Decay in E. coli," Molecules 18(3), 2712–2725 (2013).
8. A. Blázquez-Castro, "Direct $^1O_2$ optical excitation: A tool for redox biology," Redox Biology 13, 39–59 (2017).
9. C. Schweitzer, R. Schmidt, "Physical Mechanisms of Generation and Deactivation of Singlet Oxygen," Chemical Reviews 103(5), 1685–1758 (2003).
10. K. K. Wang, J. C. Finlay, T. M. Busch, S. M. Hahn, and T. C. Zhu, "Explicit dosimetry for photodynamic therapy: macroscopic singlet oxygen modeling," Journal of Biophotonics 3(5–6), 304–318 (2010).
11. A. A. Krasnovsky, "Luminescence of singlet oxygen during energy transfer from photoexcited pigments in solution," Biofizika 21, 748–755 (1976).
12. A. A. Krasnovsky, "Photoluminescence of singlet oxygen in pigment solutions," Photochemistry and Photobiology 29(1), 29–36 (1979).
13. S. Oelckers, T. Ziegler, I. Michler, and B. Röder, "Time-resolved detection of singlet oxygen luminescence in red-cell ghost suspensions: concerning a signal component that can be attributed to $^1O_2$ luminescence from the inside of a native membrane," Journal of Photochemistry and Photobiology B: Biology 53(1–3), 121–127 (1999).
14. J. G. Parker, "Optical monitoring of singlet oxygen generation during photodynamic treatment of tumors," IEEE Circuits and Devices Magazine 3(1), 10–21 (1987).
15. M. S. Patterson, S. J. Madsen, and B. C. Wilson, "Experimental tests of the feasibility of singlet oxygen luminescence monitoring in vivo during photodynamic therapy," Journal of Photochemistry and Photobiology B: Biology 5(1), 69–84 (1990).
16. M. Niedre, M. S. Patterson, and B. C. Wilson, "Direct Near-infrared Luminescence Detection of Singlet Oxygen Generated by Photodynamic Therapy in Cells In Vitro and Tissues In Vivo," Photochemistry and Photobiology 75(4), 382–391 (2002).
17. T. Hirano, E. Kohno, and M. Nishiwaki, "Detection of near infrared emission from singlet oxygen in PDT with an experimental tumor bearing mouse," Journal of Japan Society for Laser Surgery and Medicine 22, 99–108 (2002)
18. M. J. Niedre, A. J. Secord, M. S. Patterson, and B. C. Wilson, "In vitro tests of the validity of singlet oxygen luminescence measurements as a dose metric in photodynamic therapy," Cancer Research 63(22), 7986–7994 (2003).
19. M. J. Niedre, C. S. Yu, M. S. Patterson, and B. C. Wilson, "Singlet oxygen luminescence as an in vivo photodynamic therapy dose metric: validation in normal mouse skin with topical amino-levulinic acid," British Journal of Cancer 92(2), 298–304 (2005).

20. J. Yamamoto, S. Yamamoto, T. Hirano, S. Li, M. Koide, E. Kohno, M. Okada, C. Inenaga, T. Tokuyama, N. Yokota, S. Terakawa, and H. Namba, "Monitoring of Singlet Oxygen Is Useful for Predicting the Photodynamic Effects in the Treatment for Experimental Glioma," Clinical Cancer Research 12(23), 7132–7139 (2006).

21. S. Lee, D. H. Vu, M. F. Hinds, S. J. Davis, A. Liang, and T. Hasan, "Pulsed diode laser-based singlet oxygen monitor for photodynamic therapy: *in vivo* studies of tumor-laden rats," Journal of Biomedical Optics 13(6), 064035 (2008).

22. N. R. Gemmell, A. McCarthy, B. Liu, M. G. Tanner, S. D. Dorenbos, V. Zwiller, M. S. Patterson, G. S. Buller, B. C. Wilson, and R. H. Hadfield, "Singlet oxygen luminescence detection with a fiber-coupled superconducting nanowire single-photon detector," Optics Express 21(4), 5005 (2013).

23. A. E. Moskalensky, T. Yu. Karogodina, A. Yu. Vorobev, and S. G. Sokolovski, "Singlet oxygen luminescence detector based on low-cost InGaAs avalanche photodiode," HardwareX 10, e00224 (2021).

24. E. Skovsen, J. W. Snyder, J. D. C. Lambert, and P. R. Ogilby, "Lifetime and Diffusion of Singlet Oxygen in a Cell," The Journal of Physical Chemistry B 109(18), 8570–8573 (2005).

25. E. F. F. Da Silva, B. W. Pedersen, T. Breitenbach, R. Toftegaard, M. K. Kuimova, L. G. Arnaut, and P. R. Ogilby, "Irradiation- and Sensitizer-Dependent Changes in the Lifetime of Intracellular Singlet Oxygen Produced in a Photosensitized Process," The Journal of Physical Chemistry B 116(1), 445–461 (2012).

26. M. Westberg, M. Bregnhøj, A. Blázquez-Castro, T. Breitenbach, M. Etzerodt, and P. R. Ogilby, "Control of singlet oxygen production in experiments performed on single mammalian cells," Journal of Photochemistry and Photobiology A: Chemistry 321, 297–308 (2016).

27. P. Morozov, M. Lukina, M. Shirmanova, A. Divochiy, V. Dudenkova, G. N. Gol'tsman, W. Becker, and V. I. Shcheslavskiy, "Singlet oxygen phosphorescence imaging by superconducting single-photon detector and time-correlated single-photon counting," Optics Letters 46(6), 1217 (2021).

28. S. Hackbarth, W. Islam, J. Fang, V. Subr, B. Röder, T. Etrych, and H. Maeda, "Singlet oxygen phosphorescence detection *in vivo* identifies PDT-induced anoxia in solid tumors," Photochemical & Photobiological Sciences 18(6), 1304–1314 (2019).

29. Y. You, "Chemical tools for the generation and detection of singlet oxygen," Organic & Biomolecular Chemistry 16(22), 4044–4060 (2018).

30. P. S. Hosford, N. Ninkina, V. L. Buchman, J. C. Smith, N. Marina, and S. SheikhBahaei, "Synuclein Deficiency Results in Age-Related Respiratory and Cardiovascular Dysfunctions in Mice," Brain Sciences 10(9), 583 (2020).

31. S. Kim, T. Tachikawa, M. Fujitsuka, and T. Majima, "Far-Red Fluorescence Probe for Monitoring Singlet Oxygen during Photodynamic Therapy," Journal of the American Chemical Society 136(33), 11707–11715 (2014).

32. H. Gunduz, S. Kolemen, and E. U. Akkaya, "Singlet oxygen probes: Diversity in signal generation mechanisms yields a larger color palette," Coordination Chemistry Reviews 429, 213641 (2021).

33. A. Gollmer, J. Arnbjerg, F. H. Blaikie, B. W. Pedersen, T. Breitenbach, K. Daasbjerg, M. Glasius, and P. R. Ogilby, "Singlet Oxygen Sensor Green®: Photochemical Behavior in Solution and in a Mammalian Cell," Photochemistry and Photobiology 87, 671–679 (2011).

34. P. Nath, S. S. Hamadna, L. Karamchand, J. Foster, R. Kopelman, J. G. Amar, and A. Ray, "Intracellular detection of singlet oxygen using fluorescent nanosensors," Analyst 146(12), 3933–3941 (2021).

35. Z. Kadhem, S. Alkafeef, and L. Benov, "Singlet oxygen detection *in vivo* is hindered by nonspecific SOSG staining," Scientific Reports 14(1), 20669 (2024).

36. A. Prasad, M. Sedlářová, and P. Pospíšil, "Singlet oxygen imaging using fluorescent probe Singlet Oxygen Sensor Green in photosynthetic organisms," Scientific Reports 8(1), 13685 (2018).

37. I. Makovik, A. Vinokurov, A. Dunaev, E. Rafailov, and V. Dremin, "Efficiency of direct photoinduced generation of singlet oxygen at different wavelengths, power density and exposure time of laser irradiation," Analyst 148(15), 3559–3564 (2023).

38. R. Ruiz-González, R. Bresolí-Obach, Ò. Gulías, M. Agut, H. Savoie, R. W. Boyle, S. Nonell, and F. Giuntini, "NanoSOSG: A Nanostructured Fluorescent Probe for the Detection of Intracellular Singlet Oxygen," Angewandte Chemie International Edition 56(11), 2885–2888 (2017).

39. S. K. Pedersen, J. Holmehave, F. H. Blaikie, A. Gollmer, T. Breitenbach, H. H. Jensen, and P. R. Ogilby, "Aarhus Sensor Green: A Fluorescent Probe for Singlet Oxygen," The Journal of Organic Chemistry 79(7), 3079–3087 (2014).

40. T. Entradas, S. Waldron, and M. Volk, "The detection sensitivity of commonly used singlet oxygen probes in aqueous environments," Journal of Photochemistry and Photobiology B: Biology 204, 111787 (2020).

41. T. Takajo, K. Anzai, "Is There a Simple and Easy Way to Detect Singlet Oxygen? Comparison of Methods for Detecting Singlet Oxygen and Application to Measure Scavenging Activity of Various Compounds," Archives of Pharmacology and Therapeutics 2(2), (2020).

42. K. Hajdu, A. Ur Rehman, I. Vass, and L. Nagy, "Detection of Singlet Oxygen Formation inside Photoactive Biohybrid Composite Material," Materials 11(1), 28 (2017).

43. Y. Lion, M. Delmelle, and A. Van De Vorst, "New method of detecting singlet oxygen production," Nature 263(5576), 442–443 (1976).

44. D. K. Yadav, P. Pospíšil, "Evidence on the Formation of Singlet Oxygen in the Donor Side Photoinhibition of Photosystem II: EPR Spin-Trapping Study," PLoS ONE 7(9), e45883 (2012).

45. E. Koh, R. Fluhr, "Singlet oxygen detection in biological systems: Uses and limitations," Plant Signaling & Behavior 11(7), e1192742 (2016).

46. A. Mor, E. Koh, L. Weiner, S. Rosenwasser, H. Sibony-Benyamini, and R. Fluhr, "Singlet Oxygen Signatures Are Detected Independent of Light or Chloroplasts in Response to Multiple Stresses," Plant Physiology 165(1), 249–261 (2014).

47. D. M. Hodges, J. M. DeLong, C. F. Forney, and R. K. Prange, "Improving the thiobarbituric acid-reactive-substances assay for estimating lipid peroxidation in plant tissues containing anthocyanin and other interfering compounds," Planta 207(4), 604–611 (1999).

48. C. Triantaphylidès, M. Krischke, F. A. Hoeberichts, B. Ksas, G. Gresser, M. Havaux, F. Van Breusegem, and M. J. Mueller, "Singlet Oxygen Is the Major Reactive Oxygen Species Involved in Photooxidative Damage to Plants," Plant Physiology 148(2), 960–968 (2008).